Chemisorption of small fullerenes C_n ($n=28,32,36,40,44,48,60$) on the Si(001)-$c(2\times1)$ surface

Shujuan Yao,[1] Chenggang Zhou,[1] Bo Han,[1] Ting Fan,[1] Jinping Wu,[1] Liang Chen,[2] and Hansong Cheng[1]
[1]*Institute of Theoretical Chemistry and Computational Materials Science, China University of Geosciences Wuhan, Wuhan 430074, China*
[2]*Ningbo Institute of Materials Technology and Engineering, Chinese Academy of Sciences, Ningbo, Zhejiang 315201, China*
(Received 18 June 2008; revised manuscript received 19 January 2009; published 6 April 2009)

We present a systematic first-principles study using density-functional theory on chemisorption of small fullerenes C_n ($n=28,32,36,40,44,48,60$) on the Si(001)-$c(2\times1)$ reconstructed surface. The most stable adsorption structures were identified and the size-dependent adsorption strength was calculated. Detailed analysis on the geometric and electronic structures indicates that fullerenes can be strongly anchored on the substrate. Unlike adsorption of small unsaturated organic molecules on Si surfaces, where adsorption on top of Si dimers was reported to be favored, the trench channel and the two adjacent Si dimer sites were found to be the energetically preferred binding sites for fullerenes. Our results indicate that the adsorption strength is largely determined by the local curvature of fullerene molecules near the binding sites, the geometric fitness between fullerenes and adsorption sites and the stability of fullerene electronic structures. In addition, charge transfer from the substrate to fullerenes was found to be relatively small due to the highly covalent nature of the C-Si bonds formed upon fullerene chemisorption.

DOI: 10.1103/PhysRevB.79.155304 PACS number(s): 68.47.Fg, 68.43.Bc, 68.43.Fg, 68.35.bp

I. INTRODUCTION

The rapid development of microelectronic industry has presented a continued challenge for design and development of materials with desired chemical and physical properties such as low dielectric constant.[1] The ability to control the material growth plays a critical role in tailoring these properties. In the past few years, significant efforts have been made to deposit a monolayer of small unsaturated organic molecules on various semiconductor surfaces, especially silicon surfaces.[2–7] These studies have demonstrated that well-ordered organic thin films can be developed on Si surfaces via chemical reaction processes. The surface reactions are designed to take advantages of the dangling bonds of the Si surfaces and the π bonds of the unsaturated organic precursors that undergo cycloaddition reactions, similar to the Diels-Alder reactions between unsaturated organic molecules, to form ring structures between the organic molecules and the surfaces.[8–10] As a consequence, the organic molecules are tightly anchored onto the substrates, and since the reactions often occur on single-crystal surfaces, well-ordered atomistically controlled molecular deposition can be readily realized. The properties of the thin films are of course dependent on the surface substrates, specific organic molecules, and their interplays. Already, this deposition technology has found applications in optoelectronic devices, sensor technologies, and nonlinear optical materials.[11]

A number of studies have been carried out to investigate the deposition of C_{60} on Si (Refs. 12–21) and GaAs (Refs. 22–24) surfaces. Adsorption of fullerenes on Si surfaces provides a potentially important alternative to small organic molecules for tailoring properties of semiconductor materials. Earlier work of C_{60} on the Si(100)-$c(2\times1)$ surface suggested that molecular attachment to the surface is via physisorption processes.[16,17] Subsequent experimental studies suggested that C_{60} adsorption on the Si(111)-(7×7) and Si(100)-(2×1) surfaces is in fact of chemisorption nature.[18] Indeed, scanning tunneling microscopy (STM) studies have confirmed the strong interaction between fullerenes and the Si(111)-(2×1) surfaces.[19] Charge transfer from Si atoms to C_{60} molecules was deemed to occur in the deposition process.[16,20] Experimental evidence also indicates that most of the molecules can reside on the trench sites between the dimer rows at room temperature but are capable of moving up to the top of the dimer rows upon heating.[21] Significant theoretical efforts have also been made to investigate the interactions between C_{60} and Si surfaces.[25–29] Earlier first-principles calculations, however, did not consider the structural relaxations upon adsorption.[25–27] Subsequent simulations using quantum-mechanical density-functional theory (DFT) based on local-density approximation (LDA) by Godwin *et al.*[29] included the structural relaxation for both C_{60} and the surface, yielding results qualitatively consistent with experiment observations. These studies have convincingly demonstrated that strong covalent bonding interactions between fullerenes and silicon surfaces dominate the adsorption process. Nevertheless, the calculated adsorption energies appear to be overestimated due to the overbinding nature of LDA.[28,30]

Fullerenes exhibit a variety of buckyball sizes with each carbon atom adopting a pseudo-sp^2 electronic configuration. The extent of orbital distortion is largely dependent on the carbon curvature. It is thus expected that chemical reactivity of fullerenes toward Si surfaces is size dependent. Qualitatively, a fullerene with a large diameter has more flat carbon atoms and is thus anticipated to be less adhesive. In contrast, the carbon atoms in a small fullerene are more "radical-like" and thus would react with Si surfaces more strongly. The variation in adsorption strengths, coupled with a variety of sizes of fullerenes, provides an opportunity to tailor physicochemical properties of semiconductor surfaces. Unfortunately, to date, the size dependency of fullerene adsorption strength on Si surfaces has been poorly understood.

The necessity to gain quantitative understanding on adsorption properties of fullerenes of various sizes has prompted us to systematically examine adsorption of small fullerenes on the reconstructed Si(001) surface using peri-

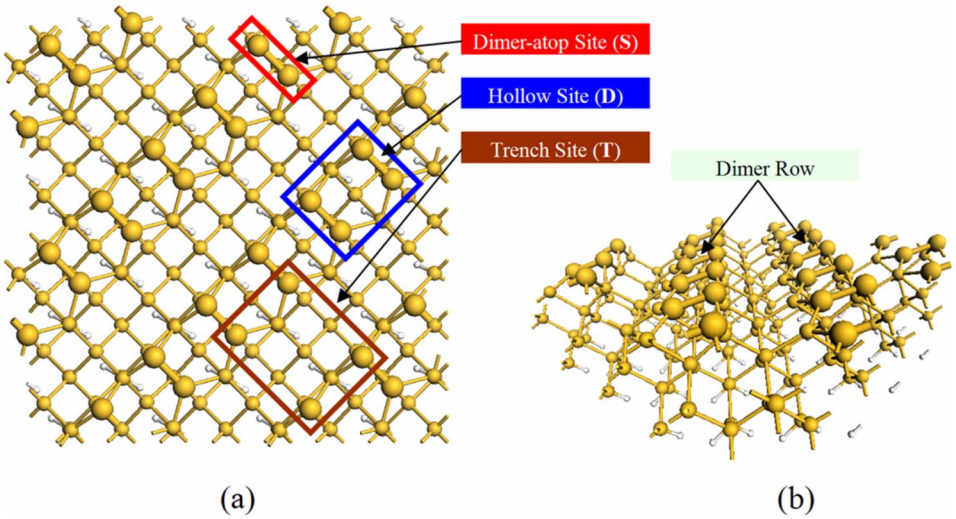

FIG. 1. (Color online) The (a) top view and (b) side view of the Si(001)-$c(2\times1)$ reconstructed surface. The three possible adsorption sites of fullerenes are marked in Fig. 1(a). The **S** site is on the top of a single dimer, the **D** site is on top of two adjacent dimers, and the **T** site is on the trench channel between two adjacent dimer rows. The top-layer dimer atoms are highlighted with large yellow (light gray) balls.

odic density-functional theory under the generalized gradient approximation (GGA). GGA has been shown in numerous studies to be highly accurate for both structures and energetics of a wide variety of surface reaction systems.[23,28] It is capable of accurately predicting the relative adsorption strengths of fullerenes on surfaces. In addition, it would be interesting to compare the similarities and differences between fullerenes and small organic molecules with π bonds upon adsorption on silicon surfaces via cycloaddition reactions. Similar to the unsaturated small organic molecules, fullerenes could react with Si surfaces via their π bonds. Potentially, both [2+2] and [4+2] cycloaddition reactions are energetically and sterically possible. Unlike the small organic molecules, however, the π orbitals in fullerenes are nearly delocalized in the entire molecule. Consequently, hexagons and pentagons on the fullerenes and their shared bonds are active and capable of participating in the cycloaddition reactions with Si dimers on the substrate. In other words, fullerenes can adopt numerous orientations to interact with the substrate using the delocalized π orbitals. Furthermore, small organic molecules with π bonds have been reportedly adsorbed only on top of a single Si dimer,[3,9,31–36] while a fullerene could be adsorbed at several active surface sites with several π bonds of the molecule participating in the surface reactions simultaneously. Obviously, the numerous fullerene orientations coupled with different binding sites drastically increase the simulation complexity.

In this paper, we present a systematic first-principles DFT study on adsorption of fullerenes C_n (n =28,32,36,40,44,48,60) on the Si(001)-$c(2\times1)$ surface. Our main purpose is to accurately describe the adsorption structures and the relative strength of fullerenes of various sizes on this important semiconductor surface. Understanding of these properties is essential for selecting appropriate sizes of fullerene molecules for deposition on the Si surface with desired adhesion strength. It is expected that Si surfaces that form strong covalent bonds with fullerenes would exhibit different properties for applications in optoelectronics.

II. COMPUTATIONAL METHODS

The Si(001) surface is one of the most well-studied systems. It undergoes significant reconstruction and exhibits several phases at various temperatures.[37–41] In this paper, we employed a slab model containing six Si layers to represent the Si(001)-$c(2\times1)$ surface. The selected supercell contains both the Si(001) slab and a fullerene molecule in a rectangular box with the cell parameters of $a=b=10.86$ Å and c =32 Å. The height of the box is sufficiently large to prevent effective interactions between slabs. The bottom Si atoms of the chosen Si(001)-$c(2\times1)$ slab are saturated with hydrogen atoms in order to terminate the dangling bonds. As shown in Fig. 1, the top-layer Si atoms are dimerized to effectively lower the surface energy and the dimer rows tilt from the surface plane. For convenience, we will denote the down-shifted Si atoms as the lower-end Si and the up-shifted Si atoms as the upper-end Si. There are three possible surface sites for fullerene adsorption, which are labeled in Fig. 1(a) as the dimer atop site (**S**), the hollow site formed by two adjacent Si dimers (**D**), and the trench site (**T**). We note in particular that the trench site is a confined channel with a width of about 5.2 Å between two Si adjacent dimer rows, and in principle, fullerene adsorption can occur by reacting with a Si dimer or two adjacent dimers at each side of the trench. The fullerenes selected in the present study include C_{28}, C_{32}, C_{36}, C_{40}, C_{44}, C_{48}, and C_{60}. Their structures were taken from our previous work.[22,23] The calculated and the experimentally available values of highest occupied molecular orbital (HOMO)-lowest unoccupied molecular orbital (LUMO) gaps and the calculated average binding energies of gas phase fullerene molecules are listed in Table I for the purpose of result analysis.

In the present study, full structural optimizations were performed for the top four layers of the substrate as well as the fullerene molecules, while the bottom two layers, together with the terminating hydrogen atoms, were kept fixed. All calculations were performed using DFT method with the

TABLE I. The calculated adsorption energy of C_n ($n=28-60$) (ΔE_{ads}) on **D** and **T** sites, charge transferred to C_n from the Si(001)-$c(2\times1)$ surface (Q), gas phase HOMO-LUMO gap (E_G^{cal} and E_G^{exp}), the maximal diameter (D_{max}), and the average binding energy (ΔE_B) of C_n.

		C_{28}	C_{32}	C_{36}	C_{40}	C_{44}	C_{48}	C_{60}
	D_{max} (Å)	4.920	5.723	5.988	6.154	6.450	7.003	7.183
	ΔE_B (eV)	6.76	6.94	6.99	7.06	7.13	7.17	7.33
	E_G^{cal} (eV)	0.27	1.40	0.37	0.95	0.90	0.68	1.79
	E_G^{exp} (eV)		1.30	0.80	0.70	0.80		1.60
T site	ΔE_{ads} (eV)	6.13	4.82	6.30	4.21	5.36	4.85	3.06
	Q (e)	0.156	0.128	0.115	0.097	0.094	0.085	0.067
D site	ΔE_{ads} (eV)	6.03	4.40	6.44	4.67	4.90	3.94	2.76
	Q (e)	0.142	0.125	0.115	0.097	0.093	0.081	0.067

exchange-correlation functional as proposed by Perdew and Wang.[42] The electron-ion interactions are described by the projector augmented wave (PAW) method,[43,44] while the valence electronic states are represented by a plane-wave basis set with a kinetic-energy cutoff of 400 eV. The Brillouin-zone integration was performed using a grid of $2\times2\times1$ Monkhorst-Pack special k points.[45] The conjugated gradient with the corrections of Blöchl *et al.*[46] was used for the geometry optimization. The computational methods used in the present study, as implemented in the Vienna *ab initio* simulation package (VASP),[47] have been shown to be highly accurate in providing reliable results on surface structure and energetic of semiconductor systems in a broad variety of studies.[28,48] Adsorption energy was calculated using the following equation:

$$E_{ads} = E(\text{sub}) + E(\text{fullerene}) - E(\text{sub} + \text{fullerene}), \quad (1)$$

where E(sub+fullerene), E(sub), and E(fullerene) are the energies of the substrate with a fullerene molecule, the substrate, and the fullerene molecule, respectively. The energies of fullerene molecules were calculated by placing them in a rigid $30\times30\times30$ Å^3 cubic box followed by full relaxation of molecular structures. The charge transfer between the fullerene molecules and the Si(001) surface was estimated using the Bader population analysis scheme.[49–51]

III. RESULTS AND DISCUSSIONS

Similar to the GaAs (001) surface,[22–24] a fullerene molecule can reside on three possible sites (**S**, **D**, and **T**) of the Si(001)-$c(2\times1)$ surface with different orientations. On each adsorption site, the bonding strength of an individual fullerene molecule was calculated by carefully examining numerous possible orientations that the molecule can adopt. A detailed description of all the possible orientations that have been sampled for the selected fullerenes would be lengthy and tedious. Instead, we will present detailed results only for C_{28}. For larger fullerenes, we will focus on adsorption at the **D** and **T** sites only since they are the dominantly preferred sites for fullerenes as will be shown later.

We first investigated C_{28} adsorption on the three binding sites on the Si(001) surface to gain insight into the relative adsorption strength. Stable adsorption structures of C_{28} can be obtained readily at the **S** and **D** sites via typical Diels-Alder type of cycloaddition reactions on the surface, similar to adsorption of many small unsaturated organic molecules.[9,52,53] Among the numerous C_{28} adsorption orientations sampled, we obtained ten stable adsorption structures with local binding modes schematically shown in Fig. 2(a) (following the schematic structural representation used by Hobbs *et al.*[28]), where the calculated adsorption energies are also labeled underneath the structures. The main calculated bond parameters are listed in Table II.

At the **S** site, the most favorable adsorption configuration is the one with a C=C bond from the hexagon undergoing a [2+2] cycloaddition with the Si-Si dimer (**S3**). C_{28} was initially placed with an edge toward a Si dimer to facilitate a [2+2] cycloaddition. Upon structural optimization, one pentagon of C_{28} leans to a **D** site, suggesting that a simple [2+2] cycloaddition between a C=C and a single Si dimer cannot stabilize the fullerene molecule. Essentially, C_{28} undergoes two pairs of [2+2] cycloaddition reactions with two adjacent surface Si dimers. One reaction is complete, forming a four-member ring with two strong C-Si covalent bonds with the bond distances of 1.967 and 2.020 Å, respectively. Another is incomplete due to the geometry ill fit between the pentagon and the two parallel Si dimers, yielding a strong C-Si covalent bond and a significantly stretched C-Si bond with bond distances of 2.006 and 3.047 Å. The adsorption gives rise to a certain degree of distortion of C_{28} structure as some of the π bonds in the molecule are readjusted. Upon the cycloaddition reaction, the C=C bond that participates the surface reaction is relaxed significantly as its bond distance changes from 1.452 to 1.60 Å. In parallel, the substrate structure is relaxed accordingly upon the adsorption. The tilted Si dimers, on which the fullerene is adsorbed, become nearly flat and the bond length is elongated by 0.03–0.08 Å. The calculated adsorption energy is 5.0 eV. The adsorption mode **S2** is less stable compared with **S3**, although it undergoes the same [2+2] cycloaddition reaction, since the additional C-Si bond is absent in this case. The weakest adsorption mode is **S1**, which undergoes a [4+2] cycloaddition. Many previous studies have suggested that the [2+2] and [4+2] cycloaddition reactions of small unsaturated organic molecules on Si(001) surface are both energeti-

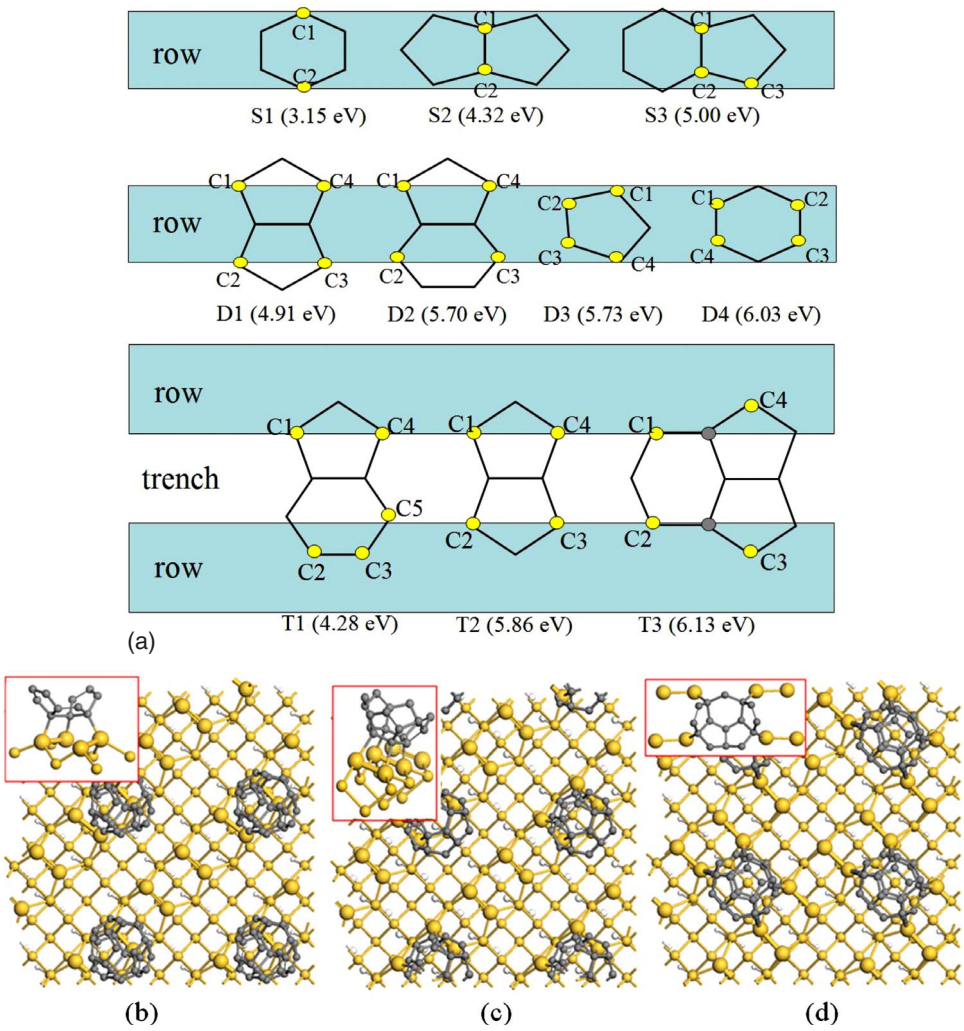

FIG. 2. (Color online) C_{28} adsorption on the Si(001)-$c(2\times1)$ reconstructed surface. (a) Schematics for **S**, **D**, and **T** configurations. The blue (gray) strips represent dimer rows. Carbon atoms that bond to Si atoms in the first layer and in the second layer are depicted as yellow (light gray) and gray circles, respectively. (b) **S3**. (c) **D4**. (d) **T3**. On each of the adsorption sites shown in (b)–(d), the local bonding structure is shown in the insets.

cally allowed but the latter is more favorable by symmetry, according to the Woodward-Hoffmann rules.[54] However, we note that in the case of small unsaturated organic molecules the π orbitals are much more localized than those in fullerenes. The highly delocalized π orbitals in fullerene molecules create more or less equal C-C bond distance and the stability of an adsorption structure strongly depends on whether the local bonding environment fits well with the Si-Si dimer structure. Therefore, despite the symmetry advantage of the [4+2] cycloaddition, the [2+2] cycloaddition in the **S3** mode is actually more preferred.

Likewise, at the **D** site, we obtained four adsorption modes. The strongest binding mode is **D4** with an adsorption energy of 6.03 eV, which corresponds to two pairs of [2+2] cycloaddition reactions. The strong adsorption preference arises from the high symmetry of the six-member ring in C_{28}, which matches well with the structure of the **D** site. C_{28} is able to adopt a symmetric orientation with a hexagon to interact effectively with two Si dimers underneath. Four C-Si bonds are formed upon the surface cycloaddition reaction, resulting in considerably stronger adhesion than at the **S** site with the calculated adsorption energy of 5.00 eV, substantially higher than the bonding strength at the S site. The optimized C-Si bond distances are 1.979, 1.980, 2.018, and 2.027 Å, respectively. Once again, slight distortion of the fullerene structure is observed and the Si(001) surface also undergoes considerable relaxation upon the adsorption. The tilted Si dimers become flat with their bond distances elongated by 0.039 and 0.040 Å, respectively. The other adsorption modes at the **D** site are generally more favorable than those at the **S** site since the C_{28} molecule forms more bonds with the substrate.

At the **T** site, the bonding structure becomes more complicated and the stability of an adsorption mode is largely dictated by the orientation of C_{28} that allows more C atoms of the molecule to interact with the surface. Among the adsorption configurations sampled, the most favorable one is that the intersection between a hexagon and two neighboring pentagons faces downward to interact with the substrate (**T3**). In addition to the formation of four covalent C-Si

TABLE II. C-Si and C-C distances (Å) of C_{28} adsorption on single dimer site (**S**), double dimer site (**D**), and trench site (**T**).

S1	C-Si	1.930	2.119				
	C1-C2	2.867→2.970					
S2	C-Si	1.929	2.046				
	C1-C2	1.527→1.636					
S3	C-Si	1.967	2.006	2.020			
	C1-C2	1.452→1.600					
D1	C-Si	1.969	2.015	1.967	2.016		
	C1-C4	2.424→2.532					
D2	C-Si	1.980	1.980	1.997	2.022		
	C1-C4	2.330→2.489					
	C2-C3	2.907→3.015					
D3	C-Si	1.992	2.012	1.999	2.086		
	C1-C4	2.525→2.510					
	C2-C3	1.638→1.629					
D4	C-Si	1.979	2.018	1.980	2.027		
	C1-C4	1.453→1.584					
T1	C-Si	1.928	1.897	1.926	2.094		
	C1-C4	2.319→2.420					
	C2-C3	1.455→1.597					
T2	C-Si	1.981	1.996	1.989	2.001		
	C1-C4	2.538→2.560					
T3	C-Si	1.957	1.959	1.993	2.003	2.524	2.544
	C1-C4	2.550→2.538					
	C1-C2	2.775→2.772					

bonds with bond lengths around 2.00 Å and two relatively weak C-Si bonds [between the C atoms and the Si atoms in the second layer, denoted by the gray circles in Fig. 2(a), with the bond lengths around 2.54 Å], more C atoms are within the vicinity of 3.755 Å of the substrate. The C_{28}-Si(001) interface is symmetric with a mirror plane. On each side of the trench channel, the end atoms of two adjacent Si dimers react with a tilted pentagon of C_{28}. Our results indicate that C_{28} is strongly anchored on the trench channel at the **T3** mode with the calculated adsorption energy of 6.13 eV. This reaction is different from the typical Diels-Alder type of cycloaddition reactions seen at the **S** and **D** sites and in many surface reactions between a Si dimer of Si(001) surface and an unsaturated small organic molecule, and it is rather unique for carbon nanostructures such as fullerenes since surface trench is also one of the energetically preferred adsorption sites for these materials. The C_{28} adsorption gives rise to significant relaxation of the surface Si dimers. The two lower-end Si atoms participating in the cycloaddition reactions at the **S** and **D** sites are slightly puckered up, while the upper-end Si atoms are considerably pushed down. As a result, the Si dimer bond lengths are elongated by 0.05–0.12 Å. In contrast, only slight structural distortion of fullerene occurs upon the chemisorption. Because of the relatively small size, C_{28} can nearly sink into the trench channel. The adsorption strength arises not only from the direct covalent bonding between C and Si atoms that participate in the trench reaction but also from the indirect but attractive interaction between C and Si atoms near the binding site. Indeed, in addition to the four strong covalent σ bonds with bond lengths of 2.00–2.05 Å formed upon fullerene chemisorption, several short Si-C distances in the range between 2.60 and 2.80 Å are also observed, as shown in the calculated Si-C distance distribution [Fig. 5(a)]. These relatively short Si-C distances also contribute to the strong adhesion strength. Bader population analysis indicates a rather small charge transfer from the substrate to C_{28} by only 0.232e, reflecting the strong covalent nature of the C-Si bonds and the higher electron affinity of C atoms.

The optimized most stable structures of C_{28} adsorbed at the **S**, **D**, and **T** sites (**S3**, **D4**, and **T3**) are displayed in Figs. 2(b)–2(d), where the local binding structures are also displayed. We note in particular that the binding strengths at the **D** and **T** sites are significantly stronger than the binding strength at the **S** site, and the calculated C_{28} adsorption energies at **D** and **T** are comparable, similar to what was found for C_{60} on Si(001) by Hobbs, *et al.*[28] It is likely that in practice the **D** and **T** sites could both be populated upon C_{28} deposition.

For other selected fullerene molecules, we similarly sampled adsorption strength at the three sites with various fullerene orientations. Without exception, we found that the

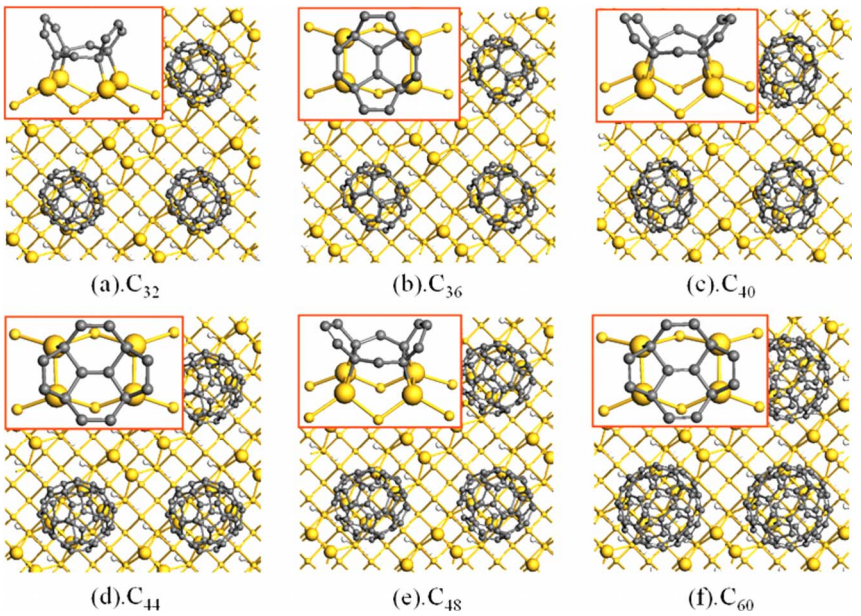

FIG. 3. (Color online) The top views of fullerenes adsorption on the **D** site of the Si(001)-$c(2\times1)$ reconstructed surface. (a) C_{32}; (b) C_{36}; (c) C_{40}; (d) C_{44}; (e) C_{48}; (f) C_{60}. The local bonding structures are displayed in the insets.

D and **T** sites are the energetically most favorable binding sites for fullerenes with comparable adsorption energies, while the local binding geometries at the interface differ from each other, depending on the initial fullerene orientations and where the fullerenes are adsorbed. Adsorption at the **S** site was found to be substantially less favorable and usually leads to adsorption at the nearby **D** site. We will therefore focus our discussions only on adsorption of the selected fullerenes at the **D** and **T** sites in this paper. The optimized adsorption structures of fullerene molecules at the energetically most favorable adhesion sites, **D** and **T**, along with their local binding geometries, are shown in Figs. 3 and 4, respectively. To qualitatively describe the bonding geometries at the fullerene-substrate interface, we show in Fig. 5 the calculated Si-C distance distributions within the range of 4.0 Å for the structures shown in Figs. 2(c), 2(d), 3, and 4. The calculated adsorption energies and the overall charges transferred from the substrate to the selected fullerene molecules are shown in Table I.

For convenience, we name the surface reaction at the **T** site as trench reaction, which always involves two adjacent Si dimers on each side of the trench. Depending on the fullerene size, these Si dimers can use the end atoms near the trench to form covalent bonds with fullerenes in the schemes shown in Fig. 6, where only the local binding areas of fullerenes are shown. In analog to the Diels-Alder type of

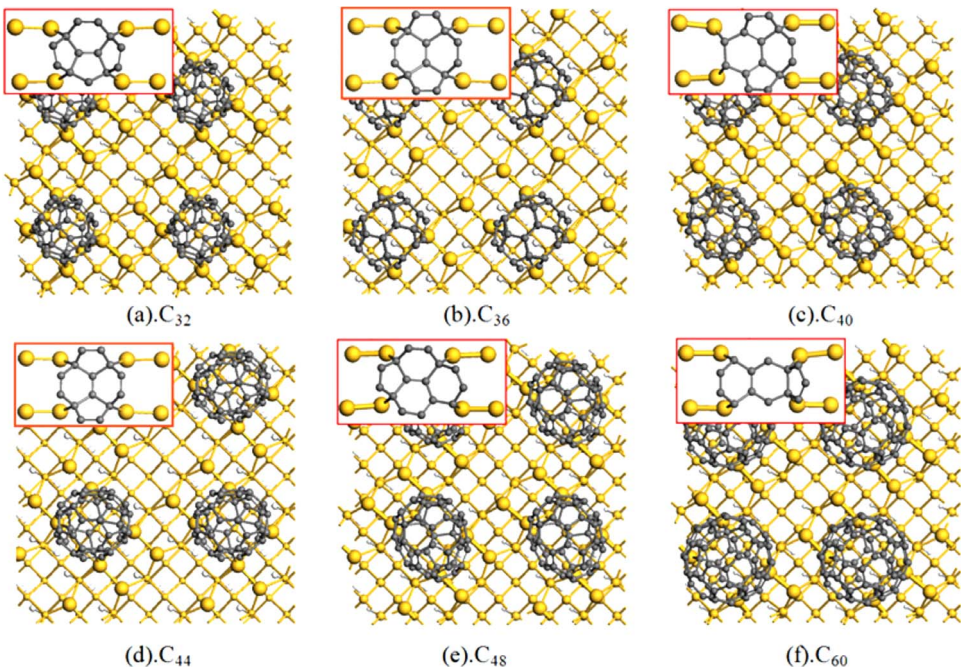

FIG. 4. (Color online) The top views of fullerenes adsorption on the **T** site of the Si(001)-$c(2\times1)$ reconstructed surface. (a) C_{32}; (b) C_{36}; (c) C_{40}; (d) C_{44}; (e) C_{48}; (f) C_{60}. The local bonding structures are displayed in the insets.

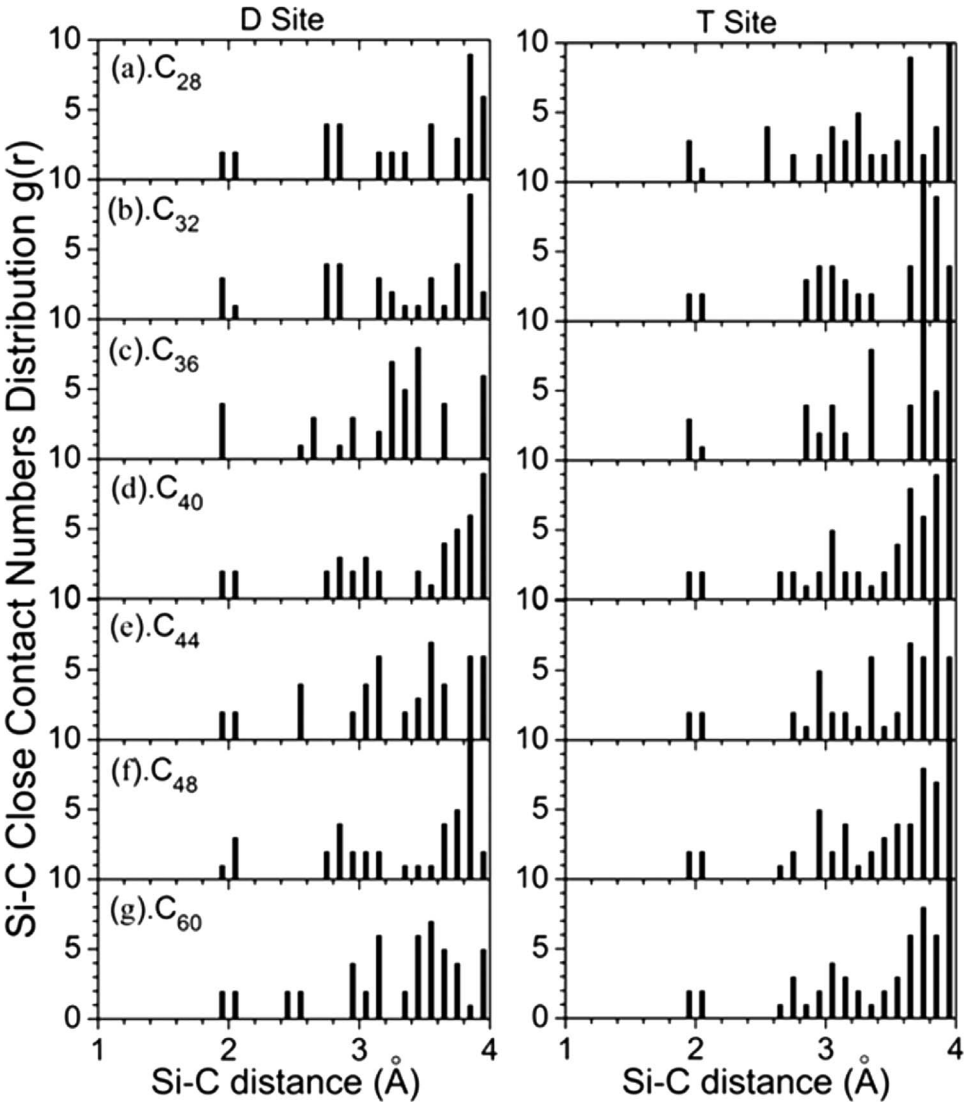

FIG. 5. The calculated Si-C bond distance distribution. (a) C_{28}. (b) C_{32}. (c) C_{36}. (d) C_{40}. (e) C_{44}. (f) C_{48}. (g) C_{60}.

cycloaddition reactions, we label the trench reactions involving two C and four C atoms as $[T+2]$ and $[T+4]$ reactions, respectively.

We then consider the adsorption structures and energetics of C_{32} on the Si(001) surface. At the **D** site, the energetically preferred adsorption structure, shown in Fig. 3(a), is similar to C_{28} on the substrate. Four C-Si bonds are formed upon two pairs of surface cycloaddition reaction with the calculated adsorption energy of 4.40 eV. The optimized C-Si bond distances are 1.970, 1.993, 1.998, and 2.023 Å, respectively. The fullerene structure exhibits marginal distortion and the Si(001) surface undergoes considerable relaxation upon the adsorption. The tilted Si dimers become flat with slightly elongated bond length by about 0.045 Å. At the **T** site, the most favorable adsorption configuration is identified as the one with the intersection between a pentagon and a hexagon right on top of the trench channel, as shown in Fig. 4(a). Similar to C_{28} on the substrate, two $[T+4]$ reactions take place at the interface, forming two C-Si covalent bonds on the upper-end Si side with bond lengths of 1.994 and 2.007 Å, and another two slightly shorter C-Si covalent bonds on the lower-end Si side with the bond lengths of 1.983 and 2.059 Å, respectively. The surface relaxation upon C_{32} adsorption is also significant. The $[T+4]$ reactions result in breaking the π bonds of the Si=Si dimers. Indeed, the two Si atoms in these dimers are now associated via a single σ bond with significantly elongated bond lengths by 0.18–0.22 Å. The calculated adsorption energy is 4.82 eV, slightly stronger than at the **D** site. Although the calculated adsorption energies suggest that the adsorption at both **T** and **D** sites is stable, surprisingly, the values are much lower than those of C_{28}. Similar to the C_{32} adsorption at the GaAs(001)-$c(4\times4)$ surface,[23,24] these abnormally low adsorption energies can be attributed to the exceptional stability of C_{32} in the gas phase. As an individual molecule, C_{32} has been shown to be much more stable than other small fullerene molecules except C_{60}.[55,56] The ultraviolet photoelectron spectra of C_{32} and C_{60} exhibit unusual large HOMO-LUMO gaps of 1.3 and 1.6 eV, respectively.[23,56] In contrast, the HOMO-LUMO gaps of other fullerene molecules are much smaller, ranging from 0.70 to 0.80 eV, as shown in Table I. The large gap significantly hinders the

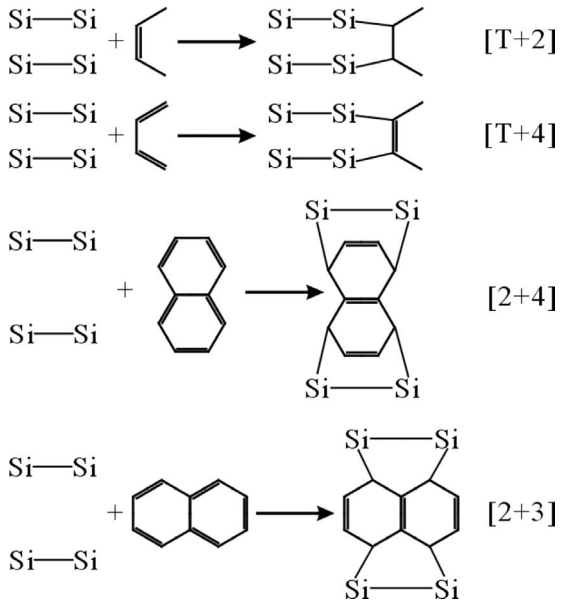

FIG. 6. The reaction schemes between surface Si dimers and fullerene molecules.

partial electron attachment to C_{32}, yielding a weaker bond strength. Indeed, the calculated charge transfer from the substrate to C_{32} is $0.139e$, which is smaller than that of C_{28}.

The structure of C_{36} molecule exhibits a high symmetry (D_{6h}). Its equator consists of six fused hexagons and each pole is composed of one hexagon. The two poles and the equator are connected by 12 pentagons, with six of them on each hemisphere. As a result, the optimized structure of C_{36} at the **D** site is also highly symmetric, as shown in Fig. 3(b). Two fused hexagons on the equator are facing downward the surface symmetrically, with the shared bond in parallel but on top of two Si dimers. Two pairs of [2+4] cycloaddition reactions take place between the two hexagons and the Si dimers. The calculated Si-C bond distances are 1.960, 1.979, 1.986, and 1.993 Å, respectively. We note that the distances between the C atoms of the shared bond and the Si atoms of the dimers are relatively short, ranging from 2.59 to 2.63 Å, adding an additional attractive force to stabilize the system. The dimer bond lengths are elongated by 0.15–0.16 Å. In particular, we found that the C_{36} structure remains nearly intact upon deposition, except that the shared edge of C_{36} is pushed upward slightly. The fused hexagon structure of C_{36} fits the Si dimers at the **D** site remarkable well, giving rise to the highest adsorption energy of 6.44 eV among the selected fullerene molecules. The charge transfer from the substrate to C_{36} is $0.113e$. At the **T** site, two fused hexagons of C_{36} on the equator are facing downward the surface, similar to the case at the **D** site as shown in the Fig. 4(b). Two $[T+4]$ reactions take place between these two hexagons and the Si dimers. The calculated Si-C bond distances are 1.972, 1.974, 1.999, and 2.002 Å, respectively. The dimer bond lengths are elongated by 0.16–0.21 Å. Again, the symmetric structure and the relatively small size of the fullerene fit well with the trench channel without significant geometric distortion. Consequently, C_{36} gains an adsorption energy of 6.302 eV, the highest among the selected fullerene molecules at the **T** site. The charge transfer from the substrate to C_{36} is $0.115e$.

The structures of C_{40}, C_{44}, and C_{48} are much less symmetric than the other fullerene molecules selected in this study. Accordingly, their adsorption structures differ significantly. The asymmetric structure prevents C_{40} from adopting a favorable orientation to interact effectively with the Si surface. At the **D** site, the adsorption structure of C_{40} adopts an orientation similar to C_{28} and C_{32}. As shown in Fig. 3(c), one hexagon is facing toward the surface dimers and interacts effectively with two adjacent Si dimers underneath via two pairs of [2+2] cycloaddition reactions. Four C-Si bonds are formed with the calculated adsorption energy of 4.67 eV, which is considerably smaller than that of C_{36} due to structural ill fit. The optimized C-Si bond distances are 1.975, 1.989, 2.051, and 2.099 Å, respectively. Slight distortion of the fullerene structure is observed and the Si(001) surface also undergoes considerable relaxation upon the adsorption. The tilted Si dimers become flat with slightly elongated bond distances by 0.03–0.04 Å. The charge transfer from the substrate to C_{40} is $0.097e$. At the **T** site, one hexagon of C_{40} is facing toward the surface trench, forming two C-Si bonds with the lower-end Si atoms with the calculated bond lengths of 1.948 and 2.005 Å, respectively, via a $[T+2]$ reaction. At the other side of the trench channel, one $[T+4]$ reaction takes place between another tilted hexagon and two upper-end Si atoms underneath, forming two uneven covalent C-Si bonds with bond lengths of 1.984 and 2.033 Å, respectively. The optimized structure at the **T** site is displayed in Fig. 4(c). Due to the structural ill fit between C_{40} and the trench channel, severe distortion of the pentagons and hexagons near the reaction sites occurs, which results in a significantly smaller adsorption energy of only 4.21 eV.

For C_{44} at the **D** site, two of the sampled adsorption orientations appear to be interesting. In both cases, two fused hexagons are oriented toward the **D** site. One is with the shared bond perpendicular to the dimers and another is with the shared bond in parallel to the dimers as illustrated schematically in Fig. 6. The calculated adsorption energies for the parallel and perpendicular orientations are 2.82 and 4.90 eV, respectively. Surprisingly, the configuration with the shared bond perpendicular to the dimers is energetically much more preferred by 2.08 eV. We note that the adsorption energy of the parallel orientation is about 3.62 eV smaller than that of C_{36} at the **D** site, although their adsorption configurations on the surface are virtually the same. This is primarily due to the fact that the bonding of C_{44} is significantly stronger than that of C_{36} in the gas phase as shown in Table I. The perpendicular orientation allows the substrate to relax more thoroughly than the parallel one with the C-Si-Si angles closer to 109° [Fig. 3(d)]. Unlike C_{36}, two pairs of [2+3] cycloaddition reactions take place between two Si dimers and two C-C-C fragments of C_{44}, forming four covalent C-Si bonds with the calculated bond lengths of 1.946, 1.955, 2.005, and 2.027 Å, respectively. The C-Si distance distribution analysis [Fig. 5(e)] indicates that the shared C=C bond is within close proximity of the Si atoms participating the bonding, ranging from 2.52 to 2.55 Å, providing additional stability. The [2+3] cycloaddition is rather unique for graphitic type of carbon materials due to the delocalization of π electrons. Likewise, the distortion of the fullerene structure is relatively

small. The tilted Si dimers become flat with significant elongated bond distance by about 0.10 Å. At the **T** site, the optimized adsorption structure of C_{44} adopts a similar orientation as that of C_{36} to interact with the Si substrate [Fig. 4(d)]. Two $[T+4]$ reactions between the tilted hexagons and Si atoms occur at both the lower-end Si side and the upper-end Si side. The calculated Si-C bond distances at the lower-end Si side are 1.958 and 1.959 Å, while the bond lengths at the upper-end Si side are 2.013 and 2.036 Å, respectively. The upstanding elliptic adsorption structure of C_{44} matches well with the trench channel, resulting in less distortion of the fullerene. As a consequence, the adsorption strength is enhanced, compared to that of C_{40}, with the calculated adsorption energy of 5.36 eV. Surface relaxation with significant Si dimer elongation, ranging from 0.191 to 0.196 Å, is observed. The calculated charge transfer to C_{44} from the substrate is 0.094 electrons.

The adsorption structure of C_{48} at the **D** site exhibits similar orientation to that of C_{40}, as shown in Fig. 3(e). Again, two pairs of $[2+2]$ cycloaddition reactions take place between a hexagon and two adjacent Si dimers. Four C-Si bonds are formed with bond lengths of 1.954, 2.038, 2.047, and 2.085 Å, respectively. The distortion of C_{48} is much greater than that of C_{40}, resulting in a significantly smaller adsorption energy of only 3.94 eV. The tilted Si dimers become rather flat with slightly elongated bond lengths by 0.03–0.04 Å and the charge transfer from the substrate to C_{48} is 0.081 e. At the **T** site, the energetically most favorable orientation is the one with two fused hexagons facing the surface with a slightly tilted configuration as shown in Fig. 4(e). One $[T+4]$ reaction takes place between a pentagon of C_{48} and two lower-end Si atoms, forming two strong covalent bonds with bond distances of about 2.03 Å. Another $[T+4]$ reaction occurs between a tilted hexagon and two Si atoms on the upper-end Si side. Both the hexagon and pentagons participating in the reactions are slightly twisted. The two relatively strong Si-C bond lengths on the upper-end side are about 2.05 Å. The calculated adsorption energy is 4.85 eV with a charge transfer of 0.085 electrons from the substrate to C_{48}.

Finally, we discuss the adsorption structure of C_{60} on the Si(001) surface. The optimized adsorption structure at the **D** site is very similar to that of C_{44}, as shown in Fig. 3(f). Two neighboring hexagons on the equator are facing downward the surface at a tilted angle, with their shared bond perpendicular to the dimers. Again, two pairs of $[2+3]$ cycloaddition reactions take place between these two hexagons and the Si dimers with bond lengths of 1.942, 1.944, 2.065, and 2.074 Å, respectively. From Fig. 5(g), it is observed that there are two nonbonding C atoms within the vicinity of the Si atoms participating the bonding. The distortion of C_{60} is relatively small and the calculated adsorption energy is 2.76 eV, which is in agreement with the previous calculation by Hobbs *et al.*[28] The Si dimers are marginally stretched by about 0.03 Å and the charge transfer from the substrate to C_{60} is $0.067e$. At the trench channel, C_{60} can be anchored with one of its hexagons facing downward and parallel to the surface. One of its neighboring hexagons is interacting with the lower-end Si atoms via a $[T+4]$ reaction. One $[T+2]$ reaction takes place on the upper-end Si side [Fig. 4(f)]. The calculated C-Si bond lengths are 1.988, 1.990, 2.044, and 2.070 Å, respectively. Due to the relatively flat structure of C_{60}, the four C atoms participating in the surface reactions have to be slightly puckered out of the original sphere to adopt a quasi-sp^3 configuration. As a result, all C-C bonds of the atoms involved in the rehybridization are elongated significantly, and the C_{60} molecule thus expands by roughly 0.26 Å in diameter. In parallel, considerable surface relaxation occurs upon C_{60} deposition. The buckled dimers involved in the bonding become rather flat and move downward with the bond lengths stretched by 0.09–0.17 Å. The significant structural distortion at the interface, coupled with the exceptionally stable electronic structure of C_{60} with a remarkably large HOMO-LUMO gap of 1.60 eV, gives rise to a relatively weak adhesion strength for C_{60} with a calculated adsorption energy of only 3.06 eV. Hobbs *et al.*[28] also examined C_{60} adsorption with this configuration at the **T** site, which was identified as one of the most stable adsorption modes.[23] Bader population analysis indicates a rather small charge transfer from the substrate to C_{60} by only $0.067e$. Our results confirm that C_{60} adsorption on Si(001)-$c(2\times1)$ surface is indeed chemisorption, consistent with what was reported by Godwin *et al.*[29] However, the overbinding, resulting from their LDA calculations, is largely corrected.

At first glance, one might expect that the fullerene adsorption strength on Si surfaces should decrease as the fullerene size increases, in view of the monotonically increasing average binding energies and decreasing curvatures of fullerenes (Table I). Instead, the calculated fullerene adsorption energies do not correlate precisely with the variation in these physical properties. The main reasons are that at the adsorption sites the local binding areas of fullerenes vary with the fullerene size, and the relative stability of electronic structure of fullerenes also plays an important role in determining the adhesion strength. For example, at the **T** site, which is a confined area with a width of about 5.2 Å, the bonding environment at the local binding sites varies, as shown in Fig. 4, owing to the variation in fullerene size and curvature. In principle, if a fullerene molecule can fit well on the binding sites to form as many strong covalent bonds as possible, without twist of the hexagons and/or pentagons involved in the reactions, maximal adhesion strength can be achieved. Obviously, highly symmetric fullerene molecules, such as C_{28} and C_{36}, can take advantage of their symmetric structures and thus form favorable strong covalent bonds with the substrate without severe distortion of their gas phase structures. For larger and asymmetric fullerene molecules, due to ill fit at the interface, the loss of adhesion strength is inevitable. Indeed, our structural analysis shows that it is increasingly difficult for fullerenes to be accommodated at both the **D** and the **T** sites as their size increases. The adhesion of a large size fullerene would result in deformation of its structure as well as distortion of the Si surface at the binding sites. In particular, the bond lengths of the surface Si dimers are significantly elongated upon the fullerenes chemisorption. In addition to the local binding environment variations, some of the fullerenes, such as C_{32} and C_{60}, exhibit remarkably stable electronic structures with large HOMO-LUMO gaps, which are not size dependent and usually give rise to weak adsorption strength. It is therefore not surprising that the calculated

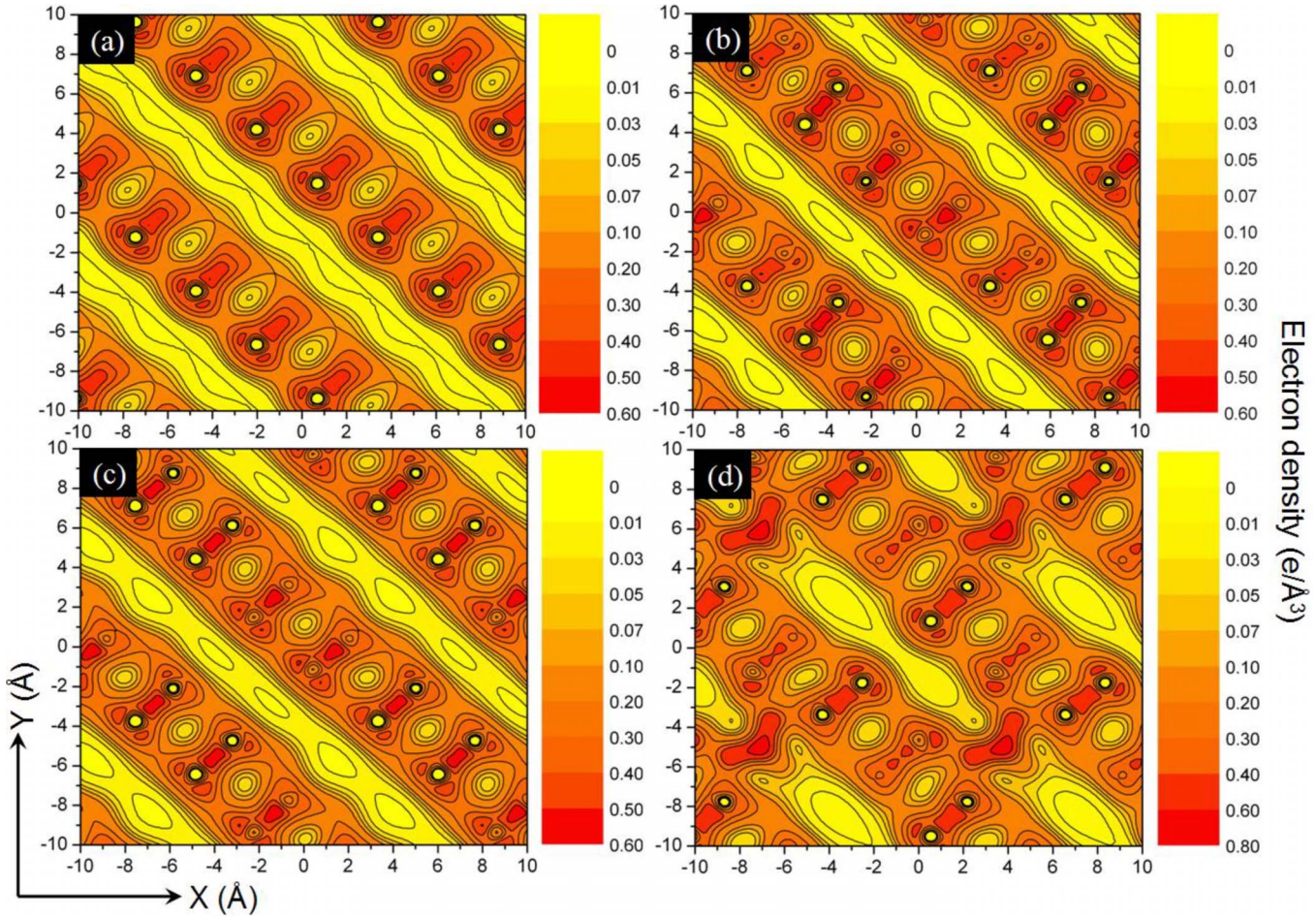

FIG. 7. (Color online) The calculated electron-density map of (a). The Si(001)-$c(2\times1)$ reconstructed surface. (b) C_{28} adsorption at the **S** site. (c) C_{28} adsorption at the **D** site; (d) C_{28} adsorption at the **T** site.

adsorption energy does not decrease monotonically with fullerene size.

Although the chemical bonds formed between fullerenes and the Si(001) surface are mainly of covalent nature, deposition of fullerenes on the Si(001) surface gives rise to charge redistribution at the interface. Figure 7 shows the calculated electron-density maps of Si(001) surface and the surface with C_{28} adsorbed at the **S**, **D**, and **T** sites, respectively. The slice was taken in the direction parallel to the surface and cutting through the center of the top-layer Si atoms. The electron-density distributions for other fullerenes on the surface exhibit similar features and thus will not be shown. For the Si(001) surface, large electron density is found around Si dimers and the trench site has the lowest electron density. The asymmetric density distribution around the Si dimers reflects the dimer tilting configurations on the substrate. Upon C_{28} adsorption at the **S** site, charge transfer from the Si dimers to the fullerene occurs, and thus the electron density on the Si atoms of the dimers (large gray balls), on which the fullerenes reside, is significantly reduced, as shown in Fig. 7(b). The upper-end Si atoms adjacent to the Si dimers, where C_{28} adsorption takes place, also appear to participate in the bonding as the electron density on these atoms decreases significantly. C_{28} adsorption at the **D** site similarly results in a considerable reduction in electron density on two pairs of neighboring Si dimers [Fig. 7(c)]. C_{28} adsorption at the **T** site leads to significant electron-density redistribution [Fig. 7(d)]. The charge depleted from the Si dimers participating in the bonding with C_{28} contributes to the large electron density in the trench areas.

Figures 8 and 9 display the calculated density of states (DOS) of the bare Si(001)-$c(2\times1)$ surface [Figs. 8(a) and 9(a)] and the surface with various sizes of fullerenes at **D** [Figs. 8(b)–8(h)] and **T** [Fig. 9(b)–9(h)] sites. For simplicity, the Fermi levels were shifted to zero. The DOS spectrum for the Si(001)-$c(2\times1)$ surface exhibits typical semiconductor characteristics with a band gap of approximately 1.1 eV. The main contributions to the conduction band and the valence band come from the $3p$ orbital of the Si atoms with a large component arising from the surface Si dimers. Upon adsorption of fullerenes, the conduction bands are somewhat broadened as the participating Si atoms are partially ionized. In all cases, strong orbital mixing between the absorbents and the substrate are observed near the Fermi level. Due to the charge transfer from the Si dimer atoms to the empty π orbitals of fullerenes, the conduction bands of the substrate are shifted downward. Again, the detail features of the DOS spectra vary with the adsorption strengths. In particular, we note that the DOS spectra of C_{36} at both the **D** and **T** sites and C_{44} at the **T** site exhibit relatively large band gaps, con-

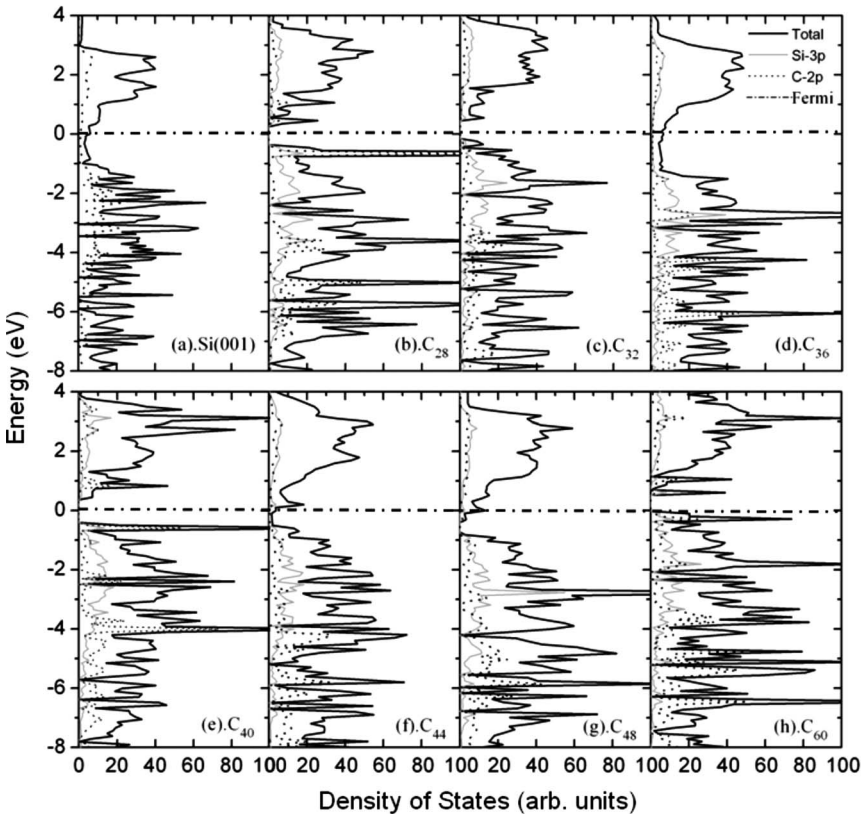

FIG. 8. The calculated DOS for the Si(001)-$c(2\times1)$ reconstructed surface and for the adsorption of fullerenes at the **D** site.

sistent with the large calculated adsorption energies. For other fullerenes, the band gaps are reduced compared with that of the Si(001) surface.

IV. SUMMARY

By depositing fullerene molecules of various sizes on selected semiconductor surfaces, materials can be tailored to achieve desired physicochemical properties, such as low dielectric constant and film thickness. Fullerenes can also be functionalized by reacting with a variety of chemical species,[57–59] which upon deposition on semiconductor surfaces can further enrich material properties. Research in this area has been of broad interest to the materials research community in recent years. It is anticipated that the morphology, uniformity, and porosity of the deposited films can be designed in a controllable manner. Hence, detailed understanding of the deposition mechanisms of fullerenes on a variety of semiconductor surfaces, such as GaAs and Si, is of essential importance. In this paper, we performed extensive first-principles studies on chemisorption of fullerene molecules, C_{28} through C_{60}, on the Si(001)-$c(2\times1)$ reconstructed surface. Because of the strained structures and extensively delocalized π orbitals, fullerenes are able to react with the surface Si dimers in various fashions to form strong covalent bonds. Adsorption of these molecules with numerous different orientations at various possible binding sites was sampled, among which the trench channels and the double dimer structures were identified to be the energetically most preferred sites. It was found that fullerene adsorption strengths at the **D** and **T** sites are in general comparable. Therefore, it is highly likely that both sites could be populated upon fullerene deposition, which is consistent with the previous report by Hobbs *et al.*[28] Recent studies on adsorption of C_{82} on the same surface by Frangou *et al.*[51] found similar adsorption preferences. Although different adsorption orientations of C_{82} could result in quite different adsorption strengths, the lowest adsorption energies of −2.84 eV at **T** sites and −3.19 eV at **D** sites are reasonably close, suggesting that both sites are capable of anchoring fullerene molecules. The fact that the trench channels are also the energetically favorable sites is significantly different from chemisorption of small unsaturated organic molecules on Si surfaces, for which the majority of studies have suggested that the unsaturated species undergo cycloaddition reactions with the surface Si dimers via the "on-top" modes (**S** or **D** site), similar to the Diels-Alder reactions.[9,52,53]

The chemical bonding of fullerenes on Si(001) surface was also found to be strikingly different from the one on GaAs(001) surface. As shown in our previous studies,[22,23] the second-layer As atoms on the GaAs(001) surface play a critical role to anchor the fullerenes on the trench sites. The dangling bonds of the second-layer As atoms make the trench sites most reactive toward fullerene deposition, while the first layer As dimers can only form relatively weaker bonding with fullerenes. In contrast, fullerene molecules are able to react more strongly with the Si surface via favorable reactions between the π bonds of fullerenes and the Si dimers both at the on-top modes and at the trench mode. In all cases, strong chemisorption occurs and covalent bonds between fullerenes and Si(001)-$c(2\times1)$ surface are formed. Bader population analysis indicates that, without exception,

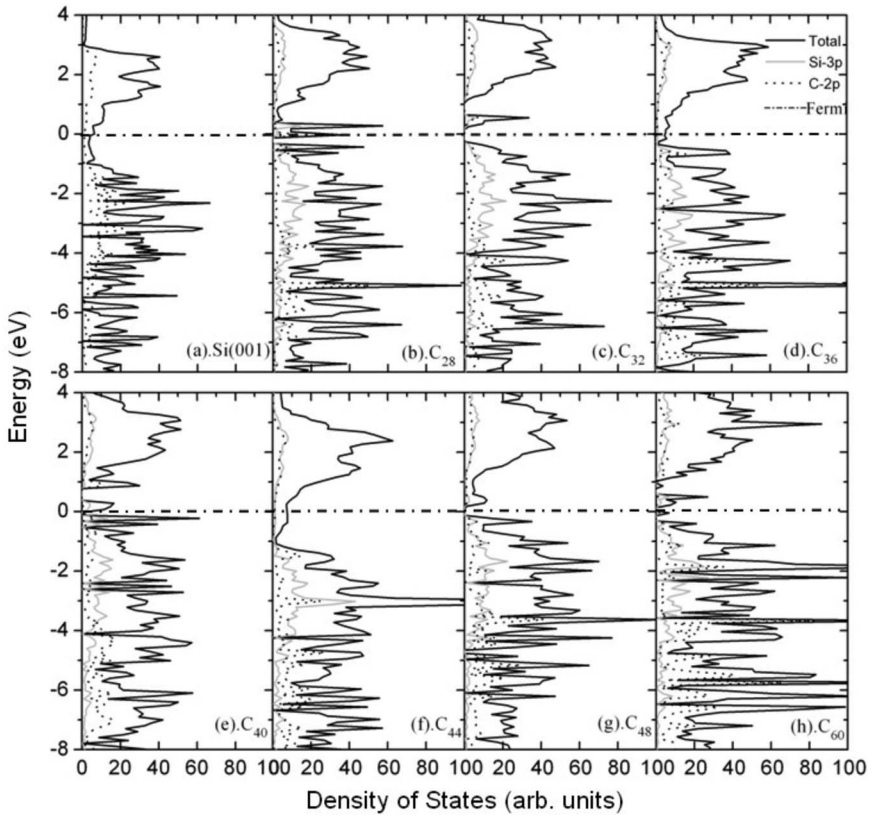

FIG. 9. The calculated DOS for the Si(001)-$c(2\times1)$ reconstructed surface and for the adsorption of fullerenes at the **T** site.

the fullerene molecules all gain a fraction of an electron from the Si(001) surface.

The major factors controlling the adhesion strength of fullerenes on the Si surface have been identified and discussed. In general, it is increasingly difficult for fullerenes to be accommodated in the **D** and **T** sites as their sizes increase. Accordingly, charge transfer from the substrate to fullerenes decays monotonically as the size of fullerenes increases. The local curvature of fullerenes near the adsorption sites dictates only the local bonding strength; a large curvature can lead to stronger bonding by relaxing the stress of the carbon atoms imposed by the quasi-sp^2 hybridization. However, the structural symmetry, stability of the fullerene molecules in the gas phase, and perhaps most importantly, the molecular orientation that allows fullerenes to fit well at the trench channels and the **D** sites to create favorable local bonding environment play a key role in determining the adhesion strength. A highly symmetric molecule can adopt an optimal orientation to effectively interact with Si dimers on both sides of trench channels and the **D** sites, while the adsorption of asymmetric molecules is usually accompanied by ill fit and significant structural distortion at the interface. The electronic density-of-states analysis indicates that these fullerene-functionalized Si surfaces exhibit considerable semiconductor or somewhat metallic characteristics. It can be anticipated that understanding of the structures and properties of fullerenes at the interface will enable us to design and develop better materials with desired properties for applications in optoelectronics.

ACKNOWLEDGMENTS

This work was supported by the National Natural Science Foundation for the Youth (Grant No. 20703040) and the Research Foundation for Outstanding Young Teachers, China University of Geosciences, Wuhan, China (Grant No. CUGQNL0519).

[1] L. Peters, Semicond. Int. **21**, 64 (1998).
[2] P. L. Silvestrelli, F. Ancilotto, and F. Toigo, Phys. Rev. B **62**, 1596 (2000).
[3] R. Konecny and D. J. Doren, Surf. Sci. **417**, 169 (1998).
[4] H. Liu and J. R. Hamers, Surf. Sci. **416**, 354 (1998).
[5] C. Huang, W. Widdra, and W. H. Weinberg, Surf. Sci. **315**, L953 (1994).
[6] C. Huang, W. Widdra, X. S. Wang, and W. H. Weinberg, J. Vac. Sci. Technol. A **11**, 2250 (1993).
[7] M. J. Bozack, P. A. Taylor, W. J. Choyke, and J. T. Yates, Surf. Sci. **177**, L933 (1986).
[8] J. Hovis, S. Lee, H. Liu, and R. J. Hamers, J. Vac. Sci. Technol. B **15**, 1153 (1997).
[9] R. J. Hamers, J. S. Hovis, S. Lee, H. Liu, and J. Shan, J. Phys. Chem. B **101**, 1489 (1997).
[10] J. S. Hovis and R. J. Hamers, J. Phys. Chem. B **101**, 9581 (1997).
[11] R. A. Wolkow, Annu. Rev. Phys. Chem. **50**, 413 (1999).

[12] H. Wang, C. Zeng, Q. Li, B. Wang, J. Yang, J. G. Hou, and Q. Zhu, Surf. Sci. **442**, L1024 (1999).
[13] K. Sakamoto, D. Kondo, M. Harada, A. Kimura, A. Kakizaki, and S. Suto, Surf. Sci. **433-435**, 642 (1999).
[14] S. Suto, K. Sakamoto, T. Wakita, M. Harada, and A. Kasuya, Surf. Sci. **402-404**, 523 (1998).
[15] K.-i. Iizumi, K. Saiki, and A. Koma, Surf. Sci. **518**, 126 (2002).
[16] S. Suto, K. Sakamoto, T. Wakita, C.-W. Hu, and A. Kasuya, Phys. Rev. B **56**, 7439 (1997).
[17] D. Chen and D. Sarid, Surf. Sci. **329**, 206 (1995).
[18] S. Suto, K. Sakamoto, D. Kondo, T. Wakita, A. Kimura, and A. Kakizaki, Surf. Sci. **427-428**, 85 (1999).
[19] J. G. Hou, Jinlong Yang, Haiqian Wang, Qunxiang Li, Changgan Zeng, Hai Lin, Wang Bing, D. M. Chen, and Qingshi Zhu, Phys. Rev. Lett. **83**, 3001 (1999).
[20] K. D. Tsuei, J. Y. Yuh, C. T. Tzeng, R. Y. Chu, S. C. Chung, and K. L. Tsang, Phys. Rev. B **56**, 15412 (1997).
[21] X. D. Wang, T. Hashizume, H. Shinohara, Y. Saito, Y. Nishina, and T. Sakurai, Phys. Rev. B **47**, 15923 (1993).
[22] S. Yao, C. Zhou, L. Ning, J. Wu, Z. Pi, H. Cheng, and Y. Jiang, Phys. Rev. B **71**, 195316 (2005).
[23] C. Zhou, J. Wu, B. Han, S. Yao, and H. Cheng, Phys. Rev. B **73**, 195324 (2006).
[24] C. Zhou, L. Ning, J. Wu, S. Yao, Z. Pi, Y. Jiang, and H. Cheng, in *Molecular Materials with Specific Interations: Modeling and Design*, edited by W. A. Sokalski (Springer, London, 2007).
[25] Y. Kawazoe, H. Kamiyama, Y. Maruyama, and K. Ohno, Jpn. J. Appl. Phys., Part 1 **32**, 1433 (1993).
[26] T. Yamaguchi, J. Vac. Sci. Technol. B **12**, 1932 (1994).
[27] A. Yajima and M. Tsukada, Surf. Sci. **357-358**, 355 (1996).
[28] C. Hobbs, L. Kantorovich, and J. D. Gale, Surf. Sci. **591**, 45 (2005).
[29] P. D. Godwin, S. D. Kenny, and R. Smith, Surf. Sci. **529**, 237 (2003).
[30] C. Hobbs and L. Kantorovich, Surf. Sci. **600**, 551 (2006).
[31] J. Yoshinobu, H. Tsuda, M. Onchi, and M. Nishijima, J. Chem. Phys. **87**, 7332 (1987).
[32] J. Yoshinobu, Y. Yamashita, F. Yasui, K. Mukai, K. Akagi, S. Tsuneyuki, K. Hamaguchi, S. Machida, M. Nagao, T. Sato, and M. Iwatsuki, J. Electron Spectrosc. Relat. Phenom. **114-116**, 383 (2001).
[33] A. V. Teplyakov, M. J. Kong, and S. F. Bent, J. Am. Chem. Soc. **119**, 11100 (1997).
[34] R. Konecny and D. J. Doren, J. Am. Chem. Soc. **119**, 11098 (1997).
[35] A. V. Teplyakov, M. J. Kong, and S. F. Bent, J. Chem. Phys. **108**, 4599 (1998).
[36] J. S. Hovis, H. B. Liu, and R. J. Hamers, J. Phys. Chem. B **102**, 6873 (1998).
[37] M. Ono, A. Kamoshida, N. Matsuura, T. E., and Y. Hasegawa, Physica B **329-333**, 1644 (2003).
[38] R. M. Tromp, R. J. Haymers, and J. E. Demuth, Phys. Rev. Lett. **55**, 1303 (1985).
[39] H. N. Waltenburg and J. Yates, Chem. Rev. **95**, 1589 (1995).
[40] T. Tabata, T. Aruga, and Y. Murata, Surf. Sci. **179**, L63 (1987).
[41] R. A. Wolkow, Phys. Rev. Lett. **68**, 2636 (1992).
[42] J. P. Perdew and Y. Wang, Phys. Rev. B **45**, 13244 (1992).
[43] P. E. Blöchl, Phys. Rev. B **50**, 17953 (1994).
[44] G. Kresse and D. Joubert, Phys. Rev. B **59**, 1758 (1999).
[45] H. J. Monkhorst and J. D. Pack, Phys. Rev. B **13**, 5188 (1976).
[46] P. E. Blöchl, O. Jepsen, and O. K. Andersen, Phys. Rev. B **49**, 16223 (1994).
[47] G. Kresse and J. Furthmüller, Phys. Rev. B **54**, 11169 (1996).
[48] C. Hobbs and L. Kantorovich, Nanotechnology **15**, S1 (2004).
[49] R. F. W. Bader, *Atoms in Molecules: A Quantum Theory* (Oxford University Press, Oxford, 1990).
[50] G. Henkelman, A. Arnaldsson, and H. Jónsson, Comput. Mater. Sci. **36**, 354 (2006).
[51] P. C. Frangou, S. D. Kenny, and E. Sanville, Surf. Sci. **602**, 1532 (2008).
[52] D. Shachal and Y. Manassen, Appl. Phys. A: Mater. Sci. Process. **66**, S1229 (1998).
[53] M. P. Schwartz, M. D. Ellison, S. K. Coulter, J. S. Hovis, and R. J. Hamers, J. Am. Chem. Soc. **122**, 8529 (2000).
[54] R. B. Woodward and R. Hoffmann, *The Conservation of Orbital Symmetry* (Academic, New York, 1970).
[55] Y. Chang, A. F. Jalbout, J. Zhang, Z. Su, and R. Wang, Chem. Phys. Lett. **428**, 148 (2006).
[56] H. Kietzmann, R. Rochow, G. Ganteför, W. Eberhardt, K. Vietze, G. Seifert, and P. W. Fowler, Phys. Rev. Lett. **81**, 5378 (1998).
[57] B. Caron, L. Derome, R. Flaminio, X. Grave, F. Marion, B. Mours, D. Verkindt, F. Cavalier, and A. Viceré, Astropart. Phys. **10**, 369 (1999).
[58] A. K. Sadana, F. Liang, B. Brinson, S. Arepalli, S. Farhat, R. H. Hauge, R. E. Smalley, and W. E. Billups, J. Phys. Chem. B **109**, 4416 (2005).
[59] T. Nakae, Y. Matsuo, and E. Nakamura, Org. Lett. **10**, 621 (2008).